

# The Chk1-mediated S-phase Checkpoint Targets Initiation Factor Cdc45 via a Cdc25A/Cdk2-independent Mechanism\*

Received for publication, March 29, 2006, and in revised form, July 31, 2006 Published, JBC Papers in Press, August 15, 2006, DOI 10.1074/jbc.M602982200

Peijun Liu<sup>‡</sup>, Laura R. Barkley<sup>‡</sup>, Tovah Day<sup>‡</sup>, Xiaohui Bi<sup>‡</sup>, Damien M. Slater<sup>‡</sup>, Mark G. Alexandrow<sup>§</sup>, Heinz-Peter Nasheuer<sup>¶</sup>, and Cyrus Vaziri<sup>‡1</sup>

From the <sup>‡</sup>Department of Genetics and Genomics, Boston University School of Medicine, Boston, Massachusetts 02118, the <sup>§</sup>H. Lee Moffitt Cancer Center & Research Institute, University of South Florida, Tampa, Florida 33612, and the <sup>¶</sup>Department of Biochemistry, Cell Cycle Control Laboratory, National University of Ireland, Galway, Ireland

DNA damage induced by the carcinogen benzo[*a*]pyrene dihydrodiol epoxide (BPDE) induces a Chk1-dependent S-phase checkpoint. Here, we have investigated the molecular basis of BPDE-induced S-phase arrest. Chk1-dependent inhibition of DNA synthesis in BPDE-treated cells occurred without detectable changes in Cdc25A levels, Cdk2 activity, or Cdc7/Dbf4 interaction. Overexpression studies showed that Cdc25A, cyclin A/Cdk2, and Cdc7/Dbf4 were not rate-limiting for DNA synthesis when the BPDE-induced S-phase checkpoint was active. To investigate other potential targets of the S-phase checkpoint, we tested the effects of BPDE on the chromatin association of DNA replication factors. The levels of chromatin-associated Cdc45 (but not soluble Cdc45) were reduced concomitantly with BPDE-induced Chk1 activation and inhibition of DNA synthesis. The chromatin association of Mcm7, Mcm10, and proliferating cell nuclear antigen was unaffected by BPDE treatment. However, the association between Mcm7 and Cdc45 in the chromatin fraction was inhibited in BPDE-treated cells. Chromatin immunoprecipitation analyses demonstrated reduced association of Cdc45 with the  $\beta$ -globin origin of replication in BPDE-treated cells. The inhibitory effects of BPDE on DNA synthesis, Cdc45/Mcm7 associations, and interactions between Cdc45 and the  $\beta$ -globin locus were abrogated by the Chk1 inhibitor UCN-01. Taken together, our results show that the association between Cdc45 and Mcm7 at origins of replication is negatively regulated by Chk1 in a Cdk2-independent manner. Therefore, Cdc45 is likely to be an important target of the Chk1-mediated S-phase checkpoint.

Cells are continuously exposed to endogenous and exogenous sources of DNA damage. Unrepaired DNA damage can cause mutations and therefore poses a serious threat to genomic stability. Cells have evolved multiple mechanisms to minimize the detrimental effects of DNA damage. Cell cycle

checkpoints are signal transduction pathways that respond to DNA damage by eliciting transient delays in the cell cycle (1). The resulting delays integrate DNA repair with cell cycle progression and are thought to be important for maintaining genomic stability. In response to genotoxins, the DNA damage response pathways prevent entry into S-phase (the G<sub>1</sub>/S checkpoint), slow progression through S-phase (the intra-S-phase or S-phase checkpoint), and block entry into mitosis (the G<sub>2</sub>/M checkpoint) (1).

Components of checkpoint signaling pathways are highly conserved in eukaryotes. DNA damage is detected by sensors (e.g. ATR/ATRIP, 9-1-1 complex, and ATM) with the aid of mediators (e.g. BRCA1, 53BP1, and Claspin). Sensors act upstream of transducers (e.g. Chk1 and Chk2), which in turn activate effectors (p53 and Cdc25A) that interact with cell cycle machinery to inhibit cell cycle progression (2).

The S-phase checkpoint down-regulates initiation of DNA synthesis in response to DNA damage acquired during S-phase (3). We characterized previously an intra-S-phase checkpoint elicited by the environmental carcinogen benzo[*a*]pyrene (4). Benzo[*a*]pyrene undergoes intracellular metabolism to generate the reactive species benzo[*a*]pyrene dihydrodiol epoxide (BPDE)<sup>2</sup> (5). BPDE reacts covalently with DNA to generate bulky adducts, mainly at *N*-2 of deoxyguanosine residues (6, 7). Different doses of BPDE inhibit DNA synthesis via distinct mechanisms. Low concentrations of BPDE (<100 nM) inhibit initiation of DNA synthesis transiently, yet do not affect elongation of existing replicons (8). Thus, the transient inhibition of DNA synthesis induced by <100 nM BPDE is an S-phase checkpoint that inhibits firing of origins of replication in response to DNA damage acquired during S-phase. We have shown that the checkpoint induced by low concentrations of BPDE is mediated via the Chk1 and 9-1-1 pathways (4, 9). Cells eventually recover from the S-phase checkpoint, and low doses of BPDE do not affect cell viability (9). However, higher concentrations of BPDE (200–600 nM) inhibit initiation and elongation steps of DNA replication, resulting in an irreversible block to DNA synthesis and loss of viability (8). The 9-1-1, Chk1, and Chk2

\* This work was supported in part by Philip Morris USA and Philip Morris International, by National Institutes of Health Grants ES09558 and ES12917 (to C. V.), and by Deutsche Forschungsgemeinschaft Grant SFB604-B2 and Health Research Board Ireland Grant RP/2003/133 (to H.-P. N.). The costs of publication of this article were defrayed in part by the payment of page charges. This article must therefore be hereby marked "advertisement" in accordance with 18 U.S.C. Section 1734 solely to indicate this fact.

<sup>1</sup> To whom correspondence should be addressed: Dept. of Genetics and Genomics, Boston University School of Medicine, 715 Albany St., E633, Boston, MA 02118. Tel.: 617-638-4175; Fax: 617-414-1646; E-mail: cvaziri@bu.edu.

<sup>2</sup> The abbreviations used are: BPDE, benzo[*a*]pyrene dihydrodiol epoxide; DSB, double-strand break; IR, ionizing radiation; GFP, green fluorescent protein; siRNA, small interfering RNA; PBS, phosphate-buffered saline; PIPES, 1,4-piperazinediethanesulfonic acid; PCNA, proliferating cell nuclear antigen; HSR, homogeneously staining region; CMV, cytomegalovirus; ChIP, chromatin immunoprecipitation; Rb, retinoblastoma; RC, replication complex.

## S-phase Checkpoint Regulation of Cdc45

pathways are strongly activated in response to 600 nM BPDE. However, the inhibition of DNA synthesis induced by 600 nM BPDE is not due to checkpoint signaling, but instead results from global blocks to the progression of DNA polymerases by BPDE adducts (8).

The dose-dependent effects of BPDE on initiation and elongation are not unique to this agent. For instance, UVC doses of  $<2.6 \text{ J/m}^2$  inhibit initiation of DNA synthesis without global effects on elongation (10), whereas higher doses inhibit both initiation and elongation. The inhibition of replicon initiation by low doses of UVC light requires ATR and Chk1 (11). Because many checkpoint studies using UVC light are conducted with high doses ( $5\text{--}100 \text{ J/m}^2$ ), it is not clear whether all the DNA damage signaling responses identified in such experiments are relevant to the S-phase checkpoint (*i.e.* inhibition of initiation) or whether they represent responses to replication blocks (inhibition of elongation).

Downstream effectors of the Chk1-mediated S-phase checkpoint induced by bulky adducts (such as BPDE and UV light-induced thymine dimers) have not been identified. However, the mechanism of the DNA double-strand break (DSB)-responsive S-phase checkpoint induced by ionizing radiation (IR) has been described in detail. There is considerable evidence that Cdc25A, a tyrosine phosphatase that contributes to activation of Cdk2 (cyclin-dependent kinase 2) (12), is targeted for degradation by IR-induced S-phase checkpoint signaling. IR-induced degradation of Cdc25A is thought to require the effector checkpoint kinases Chk1 and Chk2. Basal turnover of Cdc25A requires ATR, Claspin, and Chk1 signaling (13, 14). C-terminal phosphorylation of Cdc25A by Chk1 (together with N-terminal phosphorylation by an unknown kinase) targets Cdc25A to an SCF (Skp1-Cullin-F-box) complex containing  $\beta$ -TrCP (15–17). It is thought that the DSB-induced intra-S-phase checkpoint targets Cdc25A through Chk2-mediated amplification of Chk1-dependent systems (13, 18). Thus, loss of Chk1 results in accumulation of hypophosphorylated Cdc25A and failure to degrade Cdc25A after IR (19). The decrease in Cdk2 activity resulting from IR-induced Cdc25A degradation is likely to contribute to the S-phase checkpoint. Consistent with a Cdc25A/Cdk2-mediated mechanism for the S-phase checkpoint, the association of the Cdc45 replication factor with origins of replication (a late Cdk2-dependent event in initiation of DNA replication) is inhibited in response to IR concomitantly with Cdc25A degradation (20).

Although previous studies have demonstrated that Cdc25A is degraded in response to IR-induced DSBs (19), it is not clear whether Cdc25A is degraded in response to other forms of DNA damage such as bulky adducts or whether it represents a universal target of S-phase checkpoint signaling pathways. Moreover, as noted above, BPDE and other genotoxins elicit dose-dependent inhibition of initiation (*i.e.* the S-phase checkpoint) and inhibition of elongation (*i.e.* replication blocks), yet it is unclear if Chk1-mediated Cdc25A degradation is involved in one or both responses.

Another possible target of the S-phase checkpoint is the essential protein kinase Cdc7 (21). Cdc7 and its activating subunits (Dbf4 and Drf1) are required for DNA synthesis and appear to regulate initiation of replication at individual origins

during S-phase (22). The precise mechanism by which Cdc7 promotes initiation is not known. However, the Mcm2-7 complex is a substrate of Cdc7 *in vitro* and in intact cells (23, 24) and is likely to be involved in Cdc7-mediated initiation of DNA synthesis. Several studies have suggested that Cdc7 is a target of S-phase checkpoint signaling. For example, the *Schizosaccharomyces pombe* and *Saccharomyces cerevisiae* Dbf4 orthologs (Dfp1 and Dbf4, respectively) interact with checkpoint kinases, and yeast Dbf4 and Cdc7 mutants are sensitive to genotoxic agents (25, 26). Gautier and co-workers (27) showed that Dbf4, the activating partner of the Cdc7 kinase, is targeted by DNA damage signaling in replication-competent *Xenopus* egg extracts. In those experiments, etoposide (a topoisomerase II inhibitor) inhibited the association of Dbf4 with chromatin-bound Cdc7 concomitantly with inhibition of DNA synthesis. Furthermore, addition of exogenous Dbf4 allowed replication of etoposide-treated nuclei, demonstrating that Dbf4 is rate-limiting for DNA synthesis after etoposide treatment. Using *Xenopus* extracts, Dunphy and co-workers (28) showed that Drf1 associates with chromatin in response to DNA damage and replication stress. Therefore, these workers have suggested that Drf1 might be involved in S-phase checkpoint responses and that its association with chromatin could provide a mechanism for S-phase inhibition. However, it is not yet clear whether Cdc7/Dbf4 is targeted by S-phase checkpoint signaling in response to all genotoxins or whether Cdc7 is involved in inhibition of initiation, replication blocks, or both responses. A recent study has suggested that Dbf4 is dispensable for DNA synthesis in *Xenopus* egg extracts (29), possibly indicating a requirement for alternative Dbf4-independent mechanisms for S-phase checkpoint control.

Therefore, in the experiments described here, we investigated the possible roles of Cdc25A, Cdk2, and Cdc7/Dbf4 in the BPDE-induced S-phase checkpoint. We show that Cdc25A/Cdk2 and Cdc7/Dbf4 are affected by high doses of BPDE that inhibit elongation, but not by low doses of BPDE that induce Chk1-dependent inhibition of DNA synthesis. Consistent with these results, we show that Cdc25A/Cdk2 and Cdc7/Dbf4 are not rate-limiting for DNA synthesis in cells treated with low doses of BPDE. To identify relevant targets of the S-phase checkpoint, we tested the effects of low dose BPDE treatment on the replication factors. Our results indicate that the association between the initiation factor Cdc45 and Mcm7 is targeted by the BPDE-induced S-phase checkpoint.

## MATERIALS AND METHODS

**Cell Culture**—H1299, A549, and HeLa cells were cultured in Dulbecco's modified Eagle's medium supplemented with 10% fetal bovine serum, 100  $\mu\text{g/ml}$  streptomycin sulfate, and 100 units/ml penicillin. The Chinese hamster ovary-derived cell line A03\_1 was maintained in minimal essential medium containing 10% fetal bovine serum and 0.3  $\mu\text{M}$  methotrexate (Calbiochem).

**Adenovirus Construction and Infection**—Adenovirus construction and infections were performed as described previously (4, 30). In brief, cDNAs encoding cyclin A, Cdk2, and p21 were subcloned into pAC-CMV to generate shuttle vectors. The resulting constructs were cotransfected into 293T cells

with the pJM17 plasmid to generate recombinant adenovirus as described previously (4). H1299 cells were routinely infected with  $5 \times 10^9$  plaque-forming units/ml adenovirus. As a control for adenovirus infection, cells received an empty adenovirus vector or an adenovirus vector encoding green fluorescent protein (GFP).

**Genotoxin Treatments**—BPDE (NCI Carcinogen Repository) was dissolved in anhydrous  $\text{Me}_2\text{SO}$  and added directly to the growth medium as a 1000-fold stock solution to give the final concentrations as indicated. In some experiments, cells were incubated in medium containing 5 mM caffeine (Sigma) or 150 nM UCN-01 for 1 h before genotoxin treatment. UVC treatments were performed using a UV cross-linker (Stratagene) as described previously (31). The UVC dose delivered to the cells was confirmed with a UV radiometer (UVP Inc.).

**RNA Interference**—The non-targeting control small interfering RNA (siRNA; catalog no. D-001210-01) and human Chk1 siRNA (CHEK1, SMARTpool, catalog no. M-003255-02) oligonucleotides were obtained from Dharmacon (Lafayette, CO). siRNA transfection experiments were carried out using Lipofectamine 2000 (Invitrogen) according to the manufacturer's instructions. H1299 cells were transfected with 100 nM (final concentration) non-targeting control siRNA or Chk1 siRNA. 48 h following transfection, the cells were treated with genotoxin BPDE for 2 h, and the resulting cultures were used to analyze the expression levels of Cdc45 and Chk1.

**DNA Synthesis Assays**—Cells were plated in 12-well culture dishes and grown to 60% confluence. Genotoxin treatments were performed as described above. To measure DNA synthesis at different time points after genotoxin treatment, replicate wells received [ $^3\text{H}$ ]thymidine (1  $\mu\text{Ci}/\text{ml}$ ; PerkinElmer Life Sciences) for 30 min. At the end of the labeling period, the [ $^3\text{H}$ ]thymidine-containing medium was aspirated, and the monolayers were fixed by addition of 5% trichloroacetic acid. The fixed cells were washed three times with 5% trichloroacetic acid to remove unincorporated [ $^3\text{H}$ ]thymidine. The trichloroacetic acid-fixed cells were solubilized in 0.3 N NaOH. A 300- $\mu\text{l}$  aliquot of the NaOH-solubilized material was transferred to a scintillation vial and neutralized by addition of 100  $\mu\text{l}$  of glacial acetic acid. After addition of 5 ml of Ecoscint scintillation fluid, incorporated [ $^3\text{H}$ ]thymidine was measured by scintillation counting.

**Velocity Sedimentation Analysis**—Velocity sedimentation analysis was performed as described previously by Cordeiro-Stone *et al.* (32) with slight modifications. Briefly, H1299 cells were plated at  $5 \times 10^4$  cells/60-mm plate with two plates per condition. Following a 30-h incubation with 10 nCi/ml [ $^{14}\text{C}$ ]thymidine (to provide an internal reference for the sucrose gradient centrifugation), the radiolabeled medium was replaced with unlabeled medium for 24 h. Cells were treated with either BPDE at the indicated concentrations or  $\text{Me}_2\text{SO}$  for 1 h before pulsing with [ $^3\text{H}$ ]thymidine at 10  $\mu\text{Ci}/\text{ml}$  for 15 min. Cells were scraped into a solution of 0.1 M NaCl and 0.01 M EDTA (pH 8.0). 1 volume of 500  $\mu\text{l}$  of buffer containing 0.5 M NaOH and 0.1 M EDTA (pH 8.0) was layered on top of a linear sucrose gradient (5–20%) and 500  $\mu\text{l}$  of the cell suspension was added to this layer. Gradients were kept at 4  $^\circ\text{C}$  for 15 h under fluorescent lights and subsequently centrifuged at 25,000 rpm for 4 h at 20  $^\circ\text{C}$ . Approximately 28 equal fractions were col-

lected and acid-precipitated on glass microfiber filters. Radioactivity was determined by scintillation counting.

**Immunoblotting**—Total cell lysates were prepared in 50 mM HEPES (pH 7.4), 0.1% Triton X-100, 150 mM NaCl, 1 mM EDTA, 50 mM NaF, 80 mM  $\beta$ -glycerophosphate, and  $1 \times$  protease inhibitor mixture (Roche Applied Science). In some experiments, cells were fractionated to generate soluble fractions and whole nuclei exactly as described by Izumi *et al.* (33). In brief, monolayers of cells were washed three times with ice-cold phosphate-buffered saline (PBS) and scraped into 500  $\mu\text{l}$  of ice-cold cytoskeleton buffer (10 mM PIPES (pH 6.8), 100 mM NaCl, 300 mM sucrose, 3 mM  $\text{MgCl}_2$ , 1 mM EGTA, 1 mM dithiothreitol, 0.1 mM ATP, 1 mM  $\text{Na}_3\text{VO}_4$ , 10 mM NaF, and 0.1% Triton X-100) freshly supplemented with 0.2 mM phenylmethylsulfonyl fluoride and protease inhibitor mixture. Cytoskeleton lysates were transferred to microcentrifuge tubes and incubated on ice for 5 min. The cell lysates were centrifuged at  $1000 \times g$  for 2 min. The supernatants were removed and further clarified by centrifugation at  $10,000 \times g$  for 10 min to obtain Triton X-100-soluble fractions. The Triton X-100-extracted insoluble nuclear fractions were washed once with 1 ml of cytoskeleton buffer and then resuspended in a minimal volume of cytoskeleton buffer. In some experiments, chromatin-bound proteins were released by digestion of nuclei in cytoskeleton buffer with 1000 units/ml RNase-free DNase I (Roche Applied Science) at 25  $^\circ\text{C}$  for 30 min. After digestion, soluble and insoluble materials were separated by centrifugation at  $10,000 \times g$  for 10 min. Total cell extracts and soluble or nuclear protein samples were separated by SDS-PAGE, transferred to nitrocellulose, and analyzed by immunoblotting with the following antibodies: anti-Cdc7 (MBL International Corp.); anti-Cdc25A, anti-proliferating cell nuclear antigen (PCNA), anti-Mcm7, and anti-Chk1 (Santa Cruz Biotechnology, Inc.); anti-phospho-Chk1 and anti-phospho-Chk2 (Ser $^{317}$  and Thr $^{68}$ , respectively; Cell Signaling Technology); anti-Mcm10 (Bethyl Laboratories, Inc.); and anti-Cdc45 (34).

**Immunoprecipitations and Cdk2 Assays**—These experiments were performed exactly as described by Rosenblatt *et al.* (35). In brief, Cdk2 was immunoprecipitated from cell lysates, and the washed immune complexes were incubated with histone H1 and [ $^{32}\text{P}$ ]ATP. Phosphorylated histone was electrophoresed on SDS-polyacrylamide gels and visualized by autoradiography. To quantify Cdk2 activity, histone bands were excised from dried gels, and the amount of incorporated  $^{32}\text{P}$  was measured by Cerenkov counting.

**Chromatin Decondensation Assay**—Chromatin decondensation analyses were performed exactly as described by Alexandrow and Hamlin (36) using A03\_1 cells. A03\_1 cells contain a 90-megabase homogeneously staining region (HSR) consisting of 60 amplicons, each containing  $\sim 400$  kb of tandemly arrayed 14-kb *lac* operator/dihydrofolate reductase vector (37). The HSR can be visualized by providing the LacI protein. When visualized microscopically using an anti-Lac antibody, the HSR assumes a dot-like structure and is heterochromatic. The recruitment of Cdc45 to the HSR (using a LacI-Cdc45 fusion protein) induces a dramatic decondensation of the HSR (36). To determine the effect of checkpoint signaling on Cdc45-induced chromatin decondensation, A03\_1 cells were plated on

## S-phase Checkpoint Regulation of Cdc45

glass slides, grown to 50% confluence, and then transfected with pRcLacI or pRcLacI-Cdc45 (5  $\mu\text{g}/\text{slide}$ ) for 24 h using Lipofectamine 2000. In some experiments, cytomegalovirus (CMV)-Chk1 (or an empty vector as a control) was cotransfected at a 3:1 ratio with LacI-Cdc45. After 20 h of transfection, cells were treated with BPDE for 4 h and then washed with PBS and fixed with 4% paraformaldehyde for 10 min. After permeabilization with 0.2% Triton X-100 for 5 min, the slides were blocked with 10% fetal bovine serum and 1% bovine serum albumin in PBS for 1 h and incubated with anti-LacI monoclonal antibody (Upstate clone 9A5) at 1:2000 dilution for 1 h at room temperature. The slides were then washed with PBS containing 0.1% Tween and incubated with fluorescein isothiocyanate-conjugated goat anti-mouse IgG (Jackson ImmunoResearch Laboratories, Inc.) for 1 h. After extensive washing to remove unbound antibody, the slides were mounted with 4',6-diamidino-2-phenylindole-containing VECTASHIELD medium (Vector Laboratories) and visualized by fluorescence microscopy. To determine the relative numbers of cells containing condensed and decondensed chromatin structures, 200 cells were scored visually for each experimental condition according to the classification used by Alexandrow and Hamlin (36). The HSR was considered to be condensed if the fluorescent image occupied 2–5% of the nuclear area, decondensed if it occupied >10% of the nuclear area, and indeterminate if it occupied 5–10% of the nuclear area. Representative cells showing condensed and decondensed HSRs were photographed using a DeltaVision image restoration microscopy system (Applied Precision, LLC).

**Chromatin Immunoprecipitation (ChIP) Assays**—A 150-cm<sup>2</sup> dish of H1299 cells was used for each ChIP. Subconfluent H1299 cells were treated with or without BPDE, caffeine, and UCN-01 as indicated in the figure legends. Genotoxin-treated cells were incubated with 1% formaldehyde for 10 min to generate cross-linked DNA-protein complexes. The cross-linking reaction was quenched by addition of glycine to a final concentration of 125 mM for 10 min. The glycine-containing medium was aspirated, and the cells were washed twice with ice-cold PBS containing protease inhibitors and 1 mM phenylmethylsulfonyl fluoride. The cells were scraped into a conical tube and collected by brief centrifugation. The resulting cells were resuspended in 1 ml of 0.1 M Tris-HCl (pH 9.4) and 0.1 M dithiothreitol, placed on ice for 5 min, and incubated at 30 °C for 15 min. The cells were then collected by centrifugation and washed sequentially with 1 ml of ice-cold PBS; 1 ml of 10 mM HEPES (pH 6.5), 0.25% Triton X-100, 10 mM EDTA, and 0.5 mM EGTA; and finally 1 ml of 10 mM HEPES (pH 6.5), 1 mM EDTA, 0.5 mM EGTA, and 200 mM NaCl. The resulting cells were resuspended in 0.35 ml of buffer containing 50 mM Tris-HCl (pH 8.0), 1% SDS, and 10 mM EDTA supplemented with 1 $\times$  protease inhibitor mixture and incubated on ice for 15 min. The resulting lysates were sonicated on ice to shear the DNA into 1–2-kb fragments. Sonicated lysates were centrifuged for 10 min at 10,000  $\times$  g. The clarified supernatants containing chromatin fragments were transferred to new tubes and normalized for protein content. 5% of each sheared chromatin sample was saved to provide an “input” control. The remainder of each chromatin solution was diluted to 1 ml with 20 mM Tris-Cl (pH

8.0), 1% Triton X-100, 2 mM EDTA, and 150 mM NaCl freshly supplemented with protease inhibitor mixture. Each sample was supplemented with 400  $\mu\text{g}/\text{ml}$  salmon sperm DNA (Upstate) and 1% bovine serum albumin. Samples were then precleared with 40  $\mu\text{l}$  of a 50% protein A-agarose slurry for 4 h at 4 °C. Precleared samples were immunoprecipitated with 2–5  $\mu\text{g}$  of rabbit anti-histone H4 antibody (Upstate) as a positive control for the immunoprecipitations, rabbit preimmune serum as a negative control, or rat anti-Cdc45 monoclonal antibody (38). After overnight incubation at 4 °C, 40  $\mu\text{l}$  of pre-blocked protein G-agarose beads was added to each sample. 3 h later, immune complexes were collected by centrifugation. Beads were washed sequentially with 1 ml of buffer containing 20 mM Tris-Cl (pH 8.0), 0.1% SDS, 1% Triton X-100, 2 mM EDTA, and 150 mM NaCl; 1 ml of buffer containing 20 mM Tris-Cl (pH 8.0), 0.1% SDS, 1% Triton X-100, 2 mM EDTA, and 500 mM NaCl; 1 ml of buffer containing 10 mM Tris-Cl (pH 8.0), 0.25 M LiCl, 1% Nonidet P-40, 1% deoxycholate, and 1 mM EDTA; and finally 1 ml of Tris/EDTA buffer. Chromatin was eluted from the beads using 250  $\mu\text{l}$  of 1% SDS in 0.1 M NaHCO<sub>3</sub>. Reverse cross-linking was performed by overnight incubation at 45 °C in the presence of 10  $\mu\text{g}/\text{ml}$  proteinase K and RNase A. After phenol/chloroform extraction and ethanol precipitation, immunoprecipitated DNA was resuspended in 50  $\mu\text{l}$  of distilled water and analyzed by PCR. We synthesized PCR primers designed to amplify a 400-bp region of the  $\beta$ -globin replicator (39, 40). Identical primers were used previously to measure the association of retinoblastoma (Rb) protein with the  $\beta$ -globin origin in ChIP assays (41). The sequences of the PCR primers we used to amplify the  $\beta$ -globin locus are 5'-GAGTGAACAG-GCAACCTACAAAATGGG-3' (forward) and 5'-TCTCCAT-CCTCTCCAGCACCTG-3' (reverse). The amplified DNA products were separated on 1% agarose gels and visualized under a UV transilluminator.

**Reproducibility**—All data shown are representative of experiments that were repeated at least three times with similar results on each separate occasion.

## RESULTS

**Cdc25A and Cdk2 Are Not Targets of the BPDE-induced S-phase Checkpoint**—Chk1 mediates the S-phase checkpoint induced by low doses of BPDE (<100 nM) (4, 9). The downstream target(s) of Chk1 that mediate the S-phase checkpoint induced by bulky adducts (such as BPDE and UV light-induced thymine dimers) are not known. However, several reports have implicated Cdc25A as a target of Chk1 in the IR-induced S-phase checkpoint (13, 15, 16, 42). Therefore, we wondered whether Cdc25A is a relevant target of Chk1 in the bulky adduct-induced S-phase checkpoint resulting from BPDE treatment. We have studied regulation of DNA replication extensively in H1299 lung carcinoma cells and have shown that the BPDE-induced S-phase checkpoint is intact in this cell line (4, 30, 31, 43). Therefore, we chose H1299 cells for these experiments.

First, we determined whether the IR-induced Cdc25A degradation pathway is functional in H1299 cells. Exponentially growing H1299 cells were treated with IR (10 grays) to induce DSB as described under “Materials and Methods.” We meas-

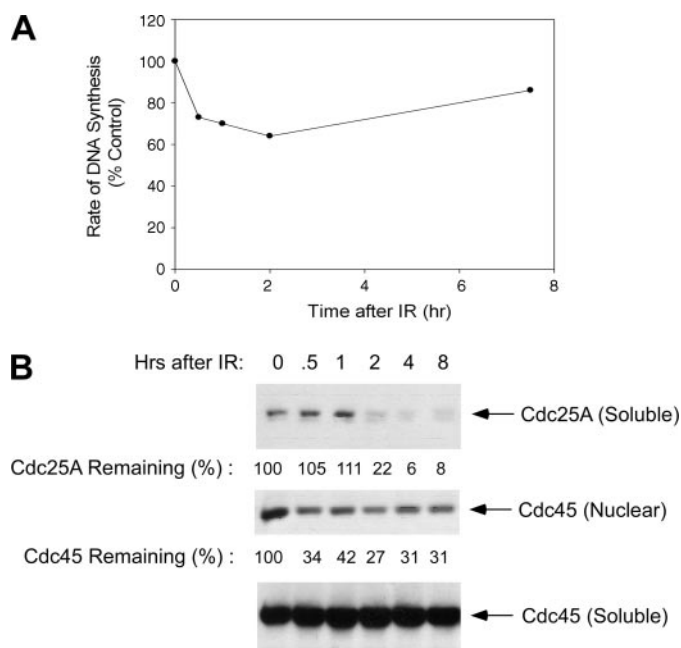


**FIGURE 1. Effect of IR on DNA synthesis and Cdc25A levels in H1299 cells.** A, exponentially growing H1299 cells were treated with 10 grays of IR. At different time points after irradiation, the rates of DNA synthesis were determined by measurements of [ $^3$ H]thymidine incorporation. B, parallel cultures of control and irradiated H1299 cells were separated to give soluble and chromatin fractions as described under "Materials and Methods." The resulting protein extracts were separated by SDS-PAGE, transferred to nitrocellulose, and probed with antibodies against Cdc25A and Cdc45.

ured the rates of DNA synthesis and Cdc25A levels in the cells at various times after irradiation. As shown in Fig. 1A, the rates of DNA synthesis (as measured by [ $^3$ H]thymidine incorporation) were reduced by  $\sim$ 30% 120 min after irradiation. Consistent with previous reports from other investigators (20, 44), the levels of Cdc25A and chromatin-associated Cdc45 were decreased concomitantly with inhibition of DNA synthesis following IR treatment (Fig. 1B). Therefore, we concluded that the IR-induced checkpoint pathway leading to Cdc25A degradation is intact in H1299 cells.

Next, we determined the effects of different doses of BPDE on DNA synthesis and Cdc25A levels. 50 nM BPDE inhibited DNA synthesis (measured by [ $^3$ H]thymidine incorporation assays) by  $\sim$ 70% for 2–4 h (Fig. 2A). However, the cells recovered from inhibition of DNA synthesis  $\sim$ 8 h after BPDE treatment (Fig. 2A). Velocity sedimentation analysis showed that 50 nM BPDE elicited a selective loss of newly initiated low molecular mass DNA (fractions 18–26 in the sedimentation profiles of Fig. 2A). In contrast, 600 nM BPDE elicited a sustained inhibition of DNA synthesis as measured by [ $^3$ H]thymidine incorporation (Fig. 2A). Velocity sedimentation analyses demonstrated that inhibition of DNA synthesis in response to 600 nM BPDE was due to loss of high molecular mass DNA (fractions 10–21 in Fig. 2A) and therefore represents reduced elongation (*i.e.* replication blocks).

Interestingly, Cdc25A levels were similar to control levels at time points when DNA synthesis was inhibited by treatment with 100 nM BPDE (Fig. 2B). However, Cdc25A expression was reduced to 42% of control levels 1 h after treatment with 600 nM BPDE. Therefore, the BPDE-induced S-phase checkpoint

(induced by low doses of BPDE) occurs without significant changes in Cdc25A levels. In contrast, high doses of BPDE that inhibit elongation reduce Cdc25A levels.

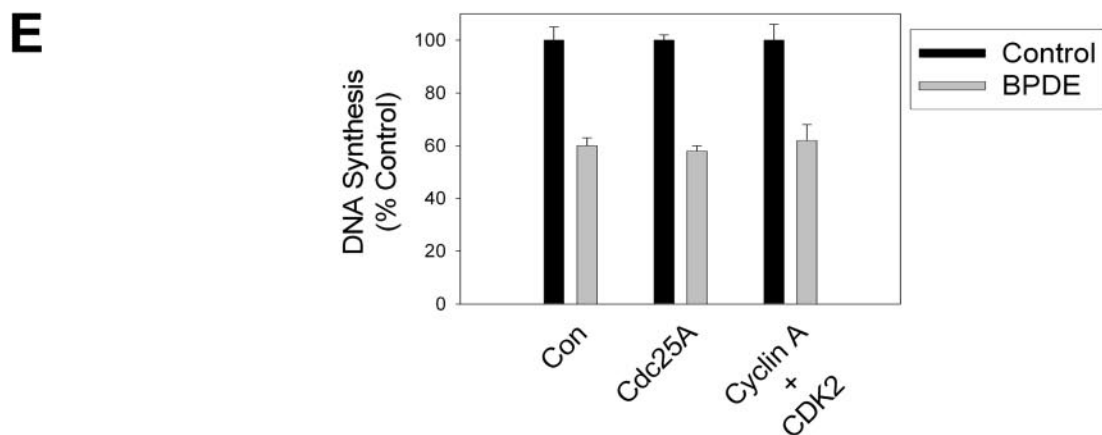
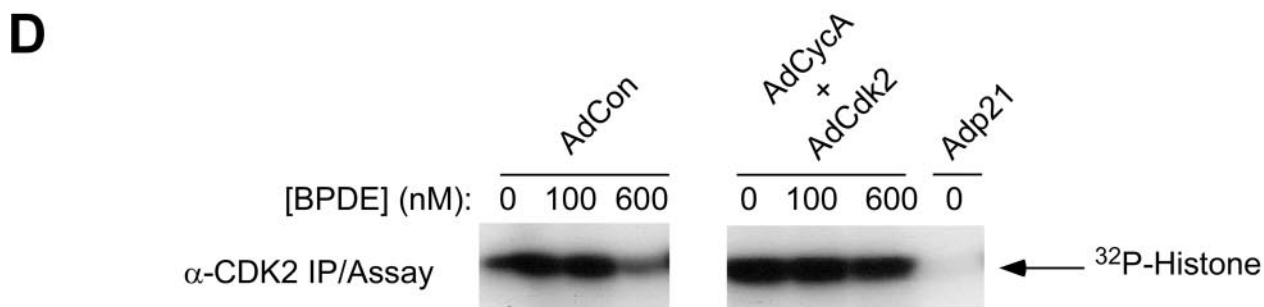
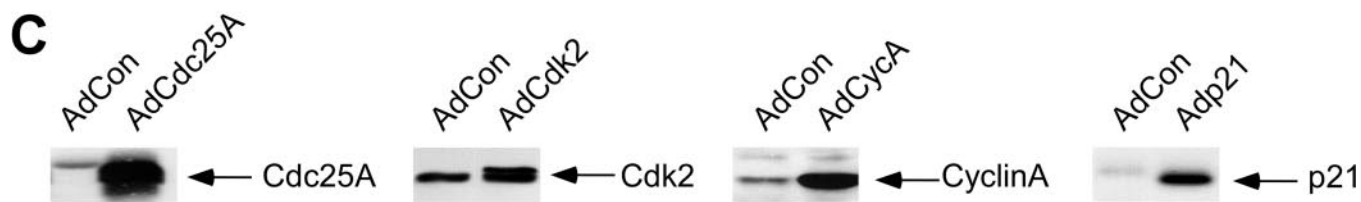
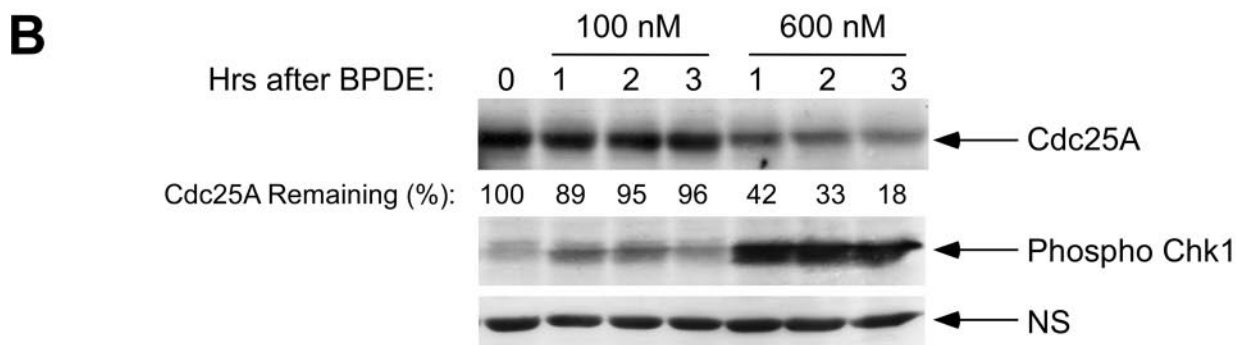
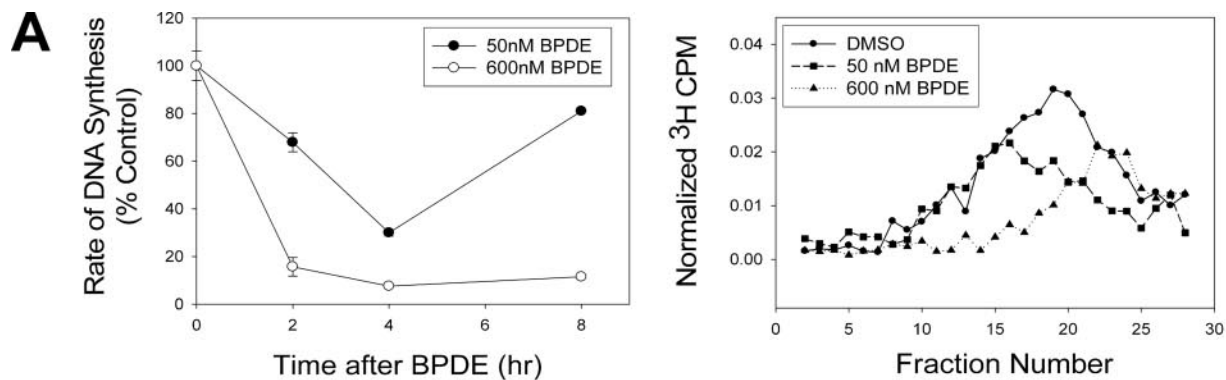
Checkpoint signaling pathways often inhibit the Cdk proteins that drive cell cycle progression. Because Cdc25A levels were unchanged in response to 100 nM BPDE, we considered the possibility that the BPDE-induced S-phase checkpoint signaling pathway might target Cdk2 activity via Cdc25A-independent mechanism(s). Therefore, we measured the histone kinase activity of immunoprecipitated Cdk2 from control and BPDE-treated cells. As shown in Fig. 2D, 100 nM BPDE had no effect on Cdk2 activity, whereas 600 nM BPDE inhibited Cdk2 by 60%. We performed parallel assays using anti-Cdk2 immunoprecipitates from cells overexpressing cyclin A and Cdk2 or from cells overexpressing p21 as positive and negative controls for these Cdk2 assays. As shown in Fig. 2D, the 600 nM BPDE-induced inhibition of Cdk2 activity was largely prevented in cells overexpressing cyclin A and Cdk2. Also as expected, overexpression of the Cdk inhibitor p21 inhibited Cdk2 activity by 95% (Fig. 2D).

The results of our Cdk2 assays were consistent with our immunoblot experiments showing that Cdc25A levels were unaffected when the BPDE-induced S-phase checkpoint was active (after treatment with  $<$ 100 nM BPDE), but that Cdc25A levels decreased in response to global replication blocks (resulting from treatment with 600 nM BPDE). Taken together, our results show that BPDE concentrations that activate the S-phase checkpoint do not affect Cdc25A levels or Cdk2 activity and that Cdc25A/Cdk2 signaling is unlikely to be a target of the S-phase checkpoint. In contrast, BPDE concentrations that induce global replication blocks inhibit both Cdc25A expression and Cdk2 activity.

It was possible that low doses of BPDE induced small changes in Cdc25A expression (or Cdk2 activity) that were undetectable in our standard assays. Potentially, even small decreases in Cdc25A expression or Cdk2 activity that were below the sensitivity level of our assays could contribute to inhibition of DNA synthesis. Therefore, to test whether Cdc25A or Cdk2 activity is rate-limiting for DNA synthesis after treatment with 100 nM BPDE, we determined the effect of ectopically expressed Cdc25A and cyclin A/Cdk2 on the S-phase checkpoint. H1299 cells were infected with adenovirus encoding Cdc25A or cyclin A/Cdk2 or with an empty control adenovirus vector. As shown in Fig. 2E, BPDE treatment inhibited DNA synthesis to a similar extent ( $\sim$ 40%) in control, Cdc25A-overexpressing, and cyclin A/Cdk2-overexpressing cells. Therefore, Cdc25A levels and cyclin A/Cdk2 activity are not rate-limiting for DNA synthesis when the BPDE-induced S-phase checkpoint is active.

**Role of Cdc7 in BPDE-induced S-phase Checkpoint Signaling—**Gautier and co-workers (27) showed that Dbf4, the activating partner of the Cdc7 kinase, is targeted by DNA damage signaling in replication-competent *Xenopus* egg extracts. In those experiments, etoposide (a topoisomerase II inhibitor) inhibited the association of Dbf4 with chromatin-bound Cdc7 concomitantly with inhibition of DNA synthesis. Furthermore, addition of exogenous Ddf4 allowed replication of etoposide-treated nuclei, demonstrating that Dbf4 is rate-limiting for DNA synthesis after etoposide treatment.

**S-phase Checkpoint Regulation of Cdc45**



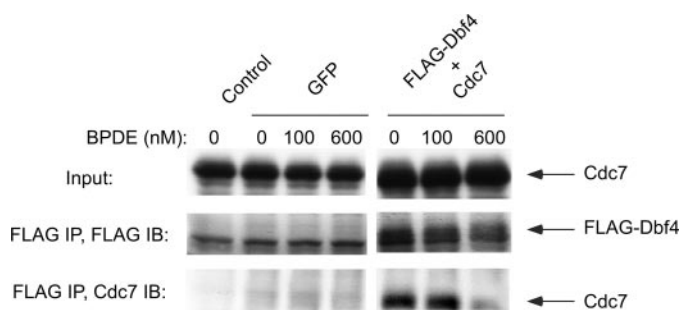


**FIGURE 3. Effect of BPDE on the association between Dbf4 and Cdc7.** Exponentially growing H1299 cells were transiently transfected with CMV-GFP or with CMV-FLAG-Dbf4 and CMV-Cdc7 as described under "Materials and Methods." Transfection efficiency was >90% as determined by immunofluorescence microscopy of GFP-transfected cultures. 48 h post-transfection, cells were treated with 100 or 600 nM BPDE for 2 h or were left untreated as a control. The resulting cells were lysed and normalized for protein concentration. An aliquot of each lysate was saved for analysis (*Input* fraction). The remainder of each extract was immunoprecipitated (*IP*) with anti-FLAG antibody. The resulting immune complexes were resolved on SDS-PAGE. Co-immunoprecipitated Cdc7 present in the anti-FLAG complexes was detected by SDS-PAGE and immunoblotting (*IB*).

Therefore, we tested a possible role for Cdc7 in the BPDE-induced S-phase checkpoint. We determined the effect of BPDE on the association between Cdc7 and Dbf4. H1299 cells were transiently transfected with CMV-FLAG-Dbf4 and CMV-Cdc7 expression vectors. As expected, Cdc7 was present in anti-FLAG immunoprecipitates from FLAG-Dbf4-expressing (but not GFP-transfected) cells (Fig. 3). We determined the effect of BPDE on the association between FLAG-Dbf4 and Cdc7. As shown in Fig. 3, FLAG-Dbf4-associated Cdc7 was readily detected in extracts from cells that did not receive BPDE. Treatment with 100 nM BPDE had no effect on the association between Dbf4 and Cdc7, demonstrating that Cdc7/Dbf4 interactions are not affected when checkpoint signaling inhibits initiation of replication. However, high doses of BPDE that inhibit elongation also reduced the association between Dbf4 and Cdc7 (Fig. 3).

Gautier and co-workers (27) showed that ectopically added Dbf4 can bypass the etoposide-induced inhibition of DNA synthesis in *Xenopus* extracts. We performed similar experiments to determine whether Dbf4 levels are rate-limiting for initiation of DNA replication after 100 nM BPDE treatment (when the S-phase checkpoint is activated). H1299 cells were transfected with a GFP expression vector as a control (and to assess transfection efficiency) or with CMV-FLAG-Dbf4. Immunofluorescence microscopy of GFP-transfected cells indicated a transfection efficiency of ~90% in these experiments. Similar to the results of Fig. 3, immunoblot analyses demonstrated that FLAG-Dbf4 was expressed efficiently in transfected cells (data

not shown). The resulting cultures were treated with BPDE for 2 h. In a representative experiment, BPDE inhibited DNA synthesis both in GFP-transfected cells and in Dbf4-overexpressing cells (42 and 39% inhibition, respectively). In other experiments, coexpression of Cdc7 with Dbf4 similarly failed to abrogate the S-phase checkpoint (data not shown). Therefore, high level expression of Dbf4 (or Dbf4 and Cdc7) does not affect the S-phase checkpoint; and in contrast with etoposide-treated *Xenopus* nuclei, Dbf4 is unlikely to be rate-limiting for DNA synthesis in H1299 cells following treatment with low or high doses of BPDE.

**Effect of BPDE on the Chromatin Association of DNA Replication Factors**—Our analyses indicated that Cdc25A, Cdk2, and Cdc7 are unlikely to be targets of the BPDE-induced S-phase checkpoint. To investigate alternative possible targets of the BPDE-induced checkpoint, we tested the effects of BPDE on DNA replication factors. During S-phase, the actions of Cdk2 and Cdc7 promote the ordered recruitment of initiation factors such as Mcm10 and Cdc45 to origins of replication (45). Cdc45 loading is one of the latest events in initiation of replication and is crucial for unwinding of origin DNA and binding of replicative DNA polymerases (a step also termed "origin firing"). In addition, a recent study has demonstrated that Cdc45 is also important for elongation (38). The chromatin association of Mcm10 and Cdc45 correlates well with initiation of DNA synthesis. For example, stimulation of origin firing by ectopic overexpression of Cdt1 in H1299 cells resulted in large increases in chromatin-associated Mcm10 and Cdc45 (Fig. 4A).

Because the BPDE-induced checkpoint inhibits initiation of replication, we sought to determine whether the chromatin association of initiation factors is sensitive to BPDE. Therefore, H1299 cells were treated with 60 or 600 nM BPDE. At different times after BPDE treatment, we determined the levels of various replication factors, including Mcm7 (a pre-replication complex (RC) component), Mcm10, Cdc45, and PCNA (a DNA polymerase processivity factor) in soluble and chromatin fractions.

As shown in Fig. 4B, the levels of chromatin-associated Mcm7, PCNA, and Mcm10 were unchanged at all times after treatment with 60 or 600 nM BPDE. However, 60 nM BPDE transiently decreased the amount of chromatin-associated Cdc45 by ~60% (Fig. 4B). The loss of chromatin-bound Cdc45 after treatment with 60 nM BPDE was coincident with Chk1 phosphorylation at Ser<sup>317</sup> and inhibition of DNA synthesis (Fig. 2A). Increased Chk2 phosphorylation (at Thr<sup>68</sup>) was not detected in response to 60 nM BPDE when initiation of DNA replication was inhibited, consistent with our previous finding

**FIGURE 2. Effect of BPDE on the rates of DNA synthesis, Cdc25A levels, and Cdk2 activity.** A, exponentially growing H1299 cells were treated with 50 or 600 nM BPDE (or were left untreated for controls). At different time points after BPDE treatment, the rates of DNA synthesis were determined by measurements of [<sup>3</sup>H]thymidine incorporation (*left panel*). For the 4-h time point, the size distribution of nascent DNAs was determined by velocity sedimentation (*right panel*). DMSO, dimethyl sulfoxide. B, H1299 cells were lysed at different time points after treatment with 100 or 600 nM BPDE. The resulting cell extracts were analyzed for Cdc25A and phospho-Chk1 (Ser<sup>317</sup>) by SDS-PAGE and immunoblotting. The band indicated by NS represents a protein that was recognized nonspecifically by anti-Chk1 antibody, which served as a loading control. C, H1299 cells were infected with AdCon, AdCdc25A, AdCdk2, AdCyclin A, or Adp21. Adenovirus-mediated overexpression of Cdc25A, Cdk2, cyclin A, and p21 was confirmed by immunoblotting of whole cell extracts. D, H1299 cells were infected with AdCon, with AdCyclin A + AdCdk2, or with Adp21. After 24 h, cells were treated with 100 nM BPDE or 600 nM for 2 h or were left untreated for controls. The cells were lysed, and Cdk2 was immunoprecipitated from the extracts. The resulting immune complexes were assayed for kinase activity against purified histone as described under "Materials and Methods." E, H1299 cells were infected with AdCon, AdCdc25A, or AdCyclin A + AdCdk2 for 24 h. Control, Cdk2 + cyclin A, and Cdc25A-overexpressing cells were treated with 100 nM BPDE or were left untreated for controls. 2 h later, rates of DNA synthesis were determined by [<sup>3</sup>H]thymidine incorporation as described under "Materials and Methods."

## S-phase Checkpoint Regulation of Cdc45

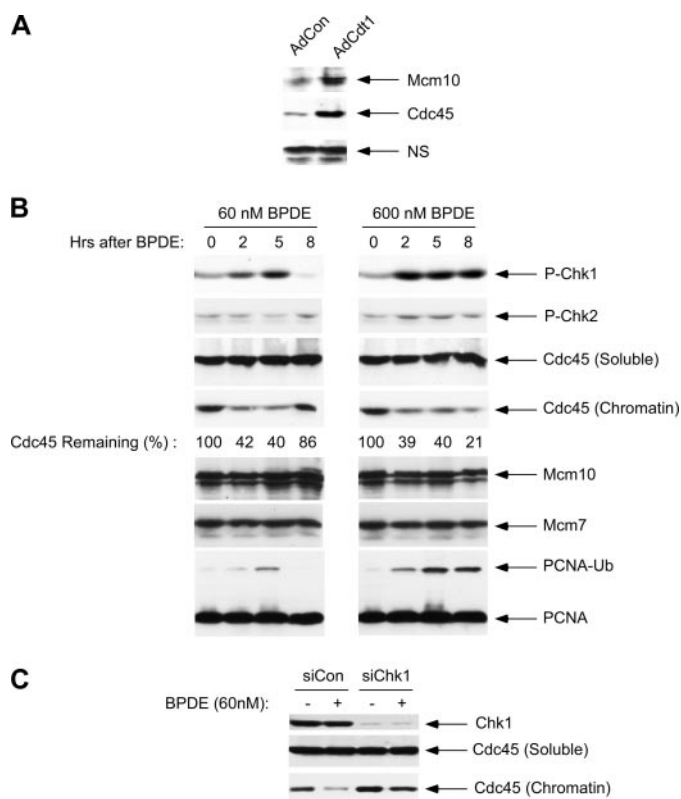


**FIGURE 4. Effect of BPDE on the chromatin association of DNA replication factors.** **A**, H1299 cells were infected with an empty control adenovirus vector (*AdCon*) or with adenovirus encoding Cdt1 (*AdCdt1*) for 24 h. The resulting cultures were separated into soluble and chromatin fractions. Washed chromatin fractions were separated by SDS-PAGE and analyzed for Cdc45 and Mcm10 levels by immunoblotting. *NS* indicates a nonspecific protein band recognized by anti-Mcm10 antibody that served as a loading control. **B**, H1299 cells were treated with 60 or 600 nM BPDE. At 0, 2, 5, and 8 h after BPDE treatment, cells were separated into soluble and chromatin fractions. After normalizing for protein, extracts were separated by SDS-PAGE and analyzed for the levels of phospho (*P*)-Chk1 (soluble fraction); phospho-Chk2 (soluble fraction); Cdc45 (chromatin and soluble fractions); and Mcm10, Mcm7, and PCNA (chromatin fractions) as described under "Materials and Methods." *PCNA-Ub*, monoubiquitinated PCNA. **C**, H1299 cells were transfected with non-targeting control siRNA (*siCon*) or Chk1 siRNA (*siChk1*). 48 h later, cells were treated with 80 nM BPDE or were left untreated as a control. After 2 h, the resulting cultures were separated into soluble and chromatin fractions. Chk1 and Cdc45 levels were detected by immunoblotting.

that the BPDE-induced S-phase checkpoint is Chk2-independent (4). 8 h after 60 nM BPDE treatment, when the rates of DNA synthesis had returned to control levels (Fig. 2A), the chromatin association of Cdc45 was also restored (Fig. 4B).

When we treated cells with 600 nM BPDE (a dose that inhibits initiation and elongation), chromatin-associated Cdc45 levels were also reduced (Fig. 4B). Both Chk1 and Chk2 were phosphorylated persistently in response to 600 nM BPDE (indicating activation of ATR/Chk1 and ATM/Chk2 pathways in response to global elongation blocks). Similar to checkpoint kinase activation and inhibition of DNA synthesis, the loss of chromatin-bound Cdc45 induced by 600 nM BPDE was irreversible (Fig. 4B). The levels of soluble Cdc45 were unaffected by BPDE, indicating that DNA damage specifically affects the chromatin-bound fraction of Cdc45 that is actively engaged in DNA replication. The levels of chromatin-bound Mcm10, Mcm7, and PCNA were also unaffected by BPDE treatment (Fig. 4B).

Therefore, BPDE concentrations as high as 600 nM do not cause a global dissociation of replication factors from chromatin.

We showed previously that Chk1 mediates BPDE-induced PCNA monoubiquitination, thereby recruiting the translesion synthesis DNA polymerase  $\kappa$  to replication forks at sites of DNA damage (43). Polymerase  $\kappa$ -mediated lesion bypass attenuates Chk1 signaling and permits resumption of DNA synthesis following checkpoint-mediated S-phase arrest (31). As shown in Fig. 4B, loss of chromatin-associated Cdc45 in BPDE-treated cells coincided with Chk1 activation and PCNA monoubiquitination. Moreover, the transient PCNA monoubiquitination induced by 60 nM BPDE preceded the re-association of Cdc45 with chromatin at 8 h. Therefore, loss of Cdc45 from chromatin after treatment with 60 nM BPDE correlates temporally with S-phase checkpoint activation. Furthermore, the re-association of Cdc45 with chromatin occurs subsequent to translesion synthesis and correlates well with the recovery phase of the S-phase checkpoint.

To test whether the BPDE-induced decrease in chromatin-bound Cdc45 is Chk1-mediated, we ablated Chk1 expression using siRNA. As shown in Fig. 4C, the BPDE-induced loss of chromatin-associated Cdc45 was largely attenuated in Chk1-depleted cells. Therefore, the BPDE-induced decrease in chromatin-associated Cdc45 requires Chk1.

Taken together, these data show that the association of Cdc45 with chromatin is sensitive to low doses of BPDE that reversibly inhibit initiation as well as high doses of BPDE that irreversibly inhibit initiation and elongation. These findings are consistent with regulation of Cdc45-chromatin association by the BPDE-induced S-phase checkpoint. As noted previously, the recruitment of Cdc45 to pre-RCs requires prior Mcm10 loading (46). Because BPDE affected the chromatin association of Cdc45 but not Mcm10, our data indicate that BPDE-induced checkpoint signaling affects initiation at a stage subsequent to Mcm10 recruitment but prior to Cdc45 loading.

*Effect of BPDE on the Association between Mcm7 and Cdc45*—Cdc45 interacts directly with Mcm7 *in vitro* and has been proposed to help tether polymerase  $\alpha$  to the RC during initiation (47). Because BPDE treatment inhibited the chromatin association of Cdc45, it was of interest to determine whether the interaction between Cdc45 and Mcm7 is disrupted concomitantly with activation of the S-phase checkpoint.

As expected, Cdc45 was immunoprecipitated with anti-Mcm7 antibody, but not with control nonspecific IgG (Fig. 5A). We performed immunoprecipitations and immunoblot analyses to determine the levels of Mcm7-associated Cdc45 in soluble and chromatin fractions at different times after BPDE treatment. As expected from the results of Fig. 4, BPDE did not affect the levels of soluble or chromatin-bound Mcm7 (Fig. 5B). However, 2 and 4 h after treatment with 60 nM BPDE, the levels of Mcm7-associated Cdc45 in chromatin fractions were decreased (by 59 and 70%, respectively) concomitantly with inhibition of DNA synthesis (Fig. 5B). At 8 h after treatment with 60 nM BPDE, the association between Cdc45 and Mcm7 in the chromatin fraction was restored to 91% of control levels concomitantly with resumption of DNA synthesis (Fig. 5B). The persistent inhibition of DNA synthesis elicited by 600 nM BPDE also induced an irreversible decrease in the interaction

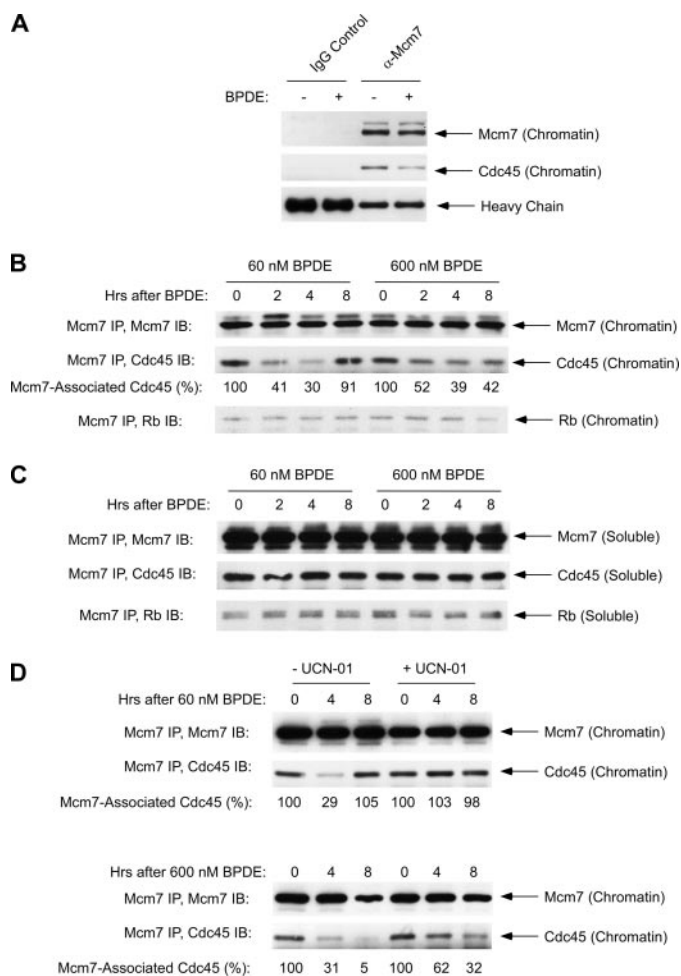


**FIGURE 5. Effect of BPDE on the interaction between Cdc45 and Mcm7.** A, H1299 cells were treated with 600 nM BPDE for 4 h or were left untreated as a control. The resulting cells were separated into soluble and chromatin fractions. After normalizing for protein content, chromatin fractions were digested with DNase I to release chromatin-associated proteins. The DNase-solubilized chromatin fractions were immunoprecipitated with anti-Mcm7 antibody or with control IgG. Immune complexes were resolved by SDS-PAGE, transferred to nitrocellulose, and probed sequentially with antibodies against Mcm7 and Cdc45. B and C, H1299 cells were treated with 60 or 600 nM BPDE. At 0, 2, 4, and 8 h after BPDE treatment, cells were separated into soluble and chromatin fractions. Chromatin-associated proteins were solubilized by DNase treatment. Then, DNase-released (B) and soluble (C) proteins were immunoprecipitated (IP) with anti-Mcm7 antibody. The resulting immune complexes were resolved by SDS-PAGE; transferred to nitrocellulose; and probed sequentially with antibodies against Cdc45, Mcm7, and Rb. IB, immunoblotting. D, H1299 cells were treated with 100 nM UCN-01 for 1 h or were left untreated. Then, control and UCN-01-treated cells received 60 or 600 nM BPDE for 0, 4, and 8 h. Chromatin fractions from the cells were harvested and digested with DNase I. Solubilized chromatin proteins were immunoprecipitated with anti-Mcm7 antibody. The resulting immunoprecipitates were resolved by SDS-PAGE, transferred to nitrocellulose, and probed with anti-Cdc45 or anti-Mcm7 antibody as indicated.

between chromatin-associated Mcm7 and Cdc45. BPDE did not affect the association between Mcm7 and Cdc45 in the soluble fraction (Fig. 5C). We considered the possibility that the effect of BPDE on Mcm7 association with Cdc45 is a general effect of DNA-damaging agents on interactions between Mcm7 and its binding partners. Mcm7 associates with the Rb tumor suppressor protein (48, 49), and this interaction has been proposed to negatively regulate DNA synthesis. We tested the effect of BPDE on the association between Mcm7 and Rb. As shown in Fig. 5 (B and C), the association between soluble or

chromatin-bound Mcm7 and Rb was unaffected by BPDE. Therefore, the inhibitory effect of BPDE on the association between Mcm7 and Cdc45 is relatively specific.

We have shown previously that the Chk1 inhibitor UCN-01 inhibits the BPDE-induced S-phase checkpoint in H1299 cells (4). To test whether the effect of BPDE on the association between Cdc45 and Mcm7 is Chk1-mediated, we determined the effect of UCN-01 on the BPDE-induced dissociation of Cdc45/Mcm7 interactions. As shown in Fig. 5D, 4 h after treatment with 60 nM BPDE, the levels of Mcm7-associated Cdc45 were decreased transiently (to 29% of control levels) and then restored 8 h after BPDE treatment when DNA synthesis resumed. In contrast, in UCN-01-treated cells, the levels of Mcm7-associated Cdc45 were unaffected by 60 nM BPDE (Fig. 5D). Therefore, UCN-01 prevents the S-phase checkpoint-mediated dissociation of Cdc45 from Mcm7.

In a parallel experiment, we determined the effect of UCN-01 on Cdc45/Mcm7 associations in cells treated with 600 nM BPDE. In contrast with the S-phase arrest induced by 60 nM BPDE, 600 nM BPDE-induced S-phase arrest is due mainly to elongation blocks and is insensitive to Chk1 inhibition (4). As shown in Fig. 5D, UCN-01 did not prevent the dissociation of Cdc45 from Mcm7 after 600 nM BPDE-induced replication blocks.

Taken together, our data suggest that Chk1 signaling inhibits DNA synthesis by targeting the interaction between Cdc45 and Mcm7 when the BPDE-induced S-phase checkpoint is active. However, replication blocks inhibit the Cdc45/Mcm7 interaction in a Chk1-independent manner.

**BPDE and Checkpoint Signaling Regulate the Association between Cdc45 and a Defined Replicator**—The S-phase checkpoint is thought to down-regulate the activities of replication origins during S-phase (3). If, as suggested by our immunoblot analyses, Cdc45 is a target of the BPDE-induced checkpoint, we predicted that the association of Cdc45 with unfired origins of DNA replication would be sensitive to DNA damage signaling. Therefore, we performed ChIPs to examine the effect of BPDE on the association between Cdc45 and a known origin of replication, *viz.* the  $\beta$ -globin locus (39).

As shown in Fig. 6A (lane 6), our anti-Cdc45 antibody (but not a control nonspecific antibody) efficiently immunoprecipitated the  $\beta$ -globin origin of replication from chromatin fractions of untreated H1299 cells. However, anti-Cdc45 immunoprecipitates of chromatin derived from cells treated with BPDE (100 or 600 nM) did not contain detectable levels of  $\beta$ -globin genomic DNA (lanes 7 and 8). Therefore, BPDE treatment prevents the association of Cdc45 with the  $\beta$ -globin origin of replication.

If the effect of BPDE on the association between Cdc45 and the  $\beta$ -globin origin results from checkpoint signaling, we predicted that inhibition of checkpoint signaling would permit the association between Cdc45 and the  $\beta$ -globin locus in BPDE-treated cells. We showed previously that caffeine (an ATR inhibitor) and UCN-01 (a Chk1 inhibitor) prevent the inhibition of DNA synthesis induced by BPDE (4). Therefore, we tested the effects of caffeine and UCN-01 on the BPDE-induced dissociation of Cdc45 from the  $\beta$ -globin locus. As expected, BPDE treatment inhibited the association between Cdc45 and

## S-phase Checkpoint Regulation of Cdc45

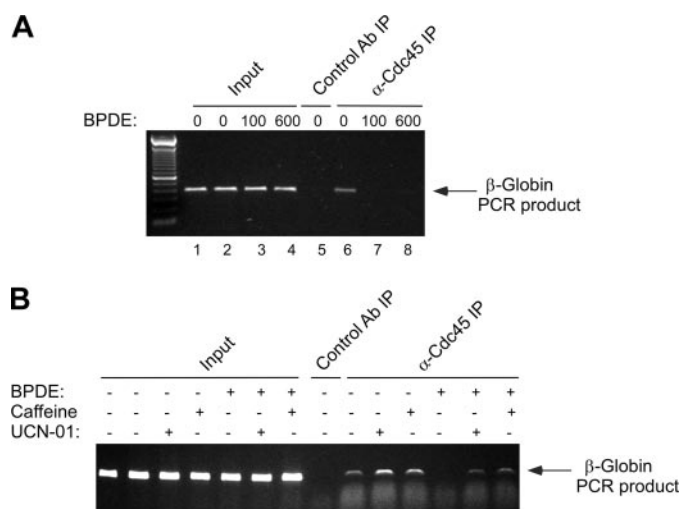


**FIGURE 6. ChIP analysis of the association between Cdc45 and the  $\beta$ -globin locus.** *A*, H1299 cells were treated with 0, 100, or 600 nM BPDE as indicated for 2 h. Cells were treated briefly with formaldehyde to cross-link DNA-protein complexes prior to harvest. Chromatin was extracted from the formaldehyde-treated cultures and sonicated to generate 1–2-kb fragments as described under “Materials and Methods.” The resulting chromatin was analyzed by PCR directly using primers designed to amplify a portion of the  $\beta$ -globin origin (*Input*) or was immunoprecipitated (*IP*) with anti-Cdc45 antibody or with control nonspecific IgG antibody (*Ab*) as a negative control prior to PCR analysis. PCR products were separated on a 1% agarose gel and visualized using ethidium bromide. *B*, H1299 cells were treated with 5 mM caffeine or 100 nM UCN-01 for 1 h or were left untreated as a control. Some of the resulting cultures were given 100 nM BPDE for an additional 2 h. Chromatin was extracted from formaldehyde-fixed cells and used in ChIP assays to detect the association between Cdc45 and the  $\beta$ -globin locus exactly as described for *A*.

the  $\beta$ -globin origin (Fig. 6*B*). Treatment with caffeine or UCN-01 alone increased the basal level of association between Cdc45 and the  $\beta$ -globin locus. This result is consistent with recent suggestions that the ATR/Chk1 pathway suppresses late origin firing and maintains ordered regulation of DNA synthesis in the absence of genotoxic insult (50). Notably, caffeine and UCN-01 treatments also allowed the association between Cdc45 and the  $\beta$ -globin origin in BPDE-treated cells (Fig. 6*B*). Therefore, inhibition of the ATR/Chk1 signaling pathway permits Cdc45 association at a defined origin of replication. Taken together, the results of our ChIP analyses are consistent with a role for Cdc45 as a target of the BPDE-induced S-phase checkpoint pathway.

**Effect of BPDE on Cdc45-induced Chromatin Decondensation**—Although Cdc45 is essential for initiation of DNA replication, its precise biochemical activity and role in DNA replication remain unclear. Recently, it was shown that targeting Cdc45 to specific chromosomal sites in A03\_1 hamster cells results in large-scale chromatin decondensation (36). Alexandrow and Hamlin (36) targeted LacI-Cdc45 (or LacI as a control) to an  $\sim$ 400-kb HSR containing multiple copies of an integrated *lac* operator/dihydrofolate reductase vector. In those experiments, the HSR was visualized by immunofluorescence microscopy with anti-LacI antibody. Ordinarily, the LacI-bound HSR assumed a condensed dot-like structure. However, targeting a LacI-Cdc45 fusion protein to the HSR resulted in dramatic chromatin decondensation (36).

Cdc45-induced chromatin decondensation might facilitate initiation of DNA synthesis and fork progression during repli-

cation (36). We hypothesized that, if Cdc45 represents a relevant target of the BPDE-induced S-phase checkpoint, its chromatin-decondensing activity might be negatively regulated by DNA damage signaling. Therefore, we tested the effects of BPDE and Chk1 on Cdc45-induced chromatin decondensation using the experimental strategy devised by Alexandrow and Hamlin (36).

First, we verified that the BPDE-induced S-phase checkpoint is intact and Cdc25A-independent in A03\_1 cells. We treated exponentially growing A03\_1 cells with 60 nM BPDE for 2 h and then measured the rates of DNA synthesis and Cdc25A levels. As shown in Fig. 7*A*, the rates of DNA synthesis were reduced by BPDE treatment, and the BPDE-induced inhibition of [ $^3$ H]thymidine incorporation was prevented by pretreatment with UCN-01. We were unable to determine the effect of BPDE on endogenous Cdc45 in A03\_1 cells because our antibody does not recognize hamster Cdc45. However, immunoblot experiments showed that the BPDE-induced inhibition of DNA synthesis occurred in the absence of changes in Cdc25A levels (Fig. 7*B*). Taken together, these results demonstrate that the BPDE-induced S-phase checkpoint is functional and independent of changes in Cdc25A expression in A03\_1 cells.

Having confirmed that the BPDE-induced S-phase checkpoint is intact in A03\_1 cells, we determined the effect of BPDE on Cdc45-induced chromatin decondensation. Fig. 7*C* shows examples of the typical condensed dot-like HSR structures seen in LacI-transfected cells (*first panels*) as well as the decondensed HSRs elicited by LacI-Cdc45 (*second panels*). As shown in Fig. 7 (*C, third panels; and D*), treatment with 100 nM BPDE reduced the number of cells containing decondensed chromatin by  $>$ 50%, indicating that BPDE inhibits Cdc45-induced chromatin decondensation. Interestingly, cotransfection of LacI-Cdc45 with a Chk1 expression vector also inhibited Cdc45-induced chromatin decondensation, even in the absence of BPDE (*fourth panels*). We have shown previously that overexpressed Chk1 induces a DNA damage-independent S-phase arrest (4). Taken together, our data demonstrate that BPDE or overexpressed Chk1 inhibits Cdc45-induced chromatin decondensation. These results are consistent with a role for Cdc45 as a target of the BPDE-induced S-phase checkpoint.

**The UVC Light-induced S-phase Checkpoint Targets Cdc45 Independently of Cdc25A**—It was of interest to determine whether the Cdc25A-independent effect of BPDE on Cdc45 is a general response to genotoxins. Similar to BPDE-induced adducts, UVC light-induced cyclobutane pyrimidine dimers inhibit initiation of DNA synthesis via Chk1 signaling (11). Therefore, we compared the S-phase checkpoint responses to BPDE- and UVC light-induced DNA damage.

We measured the rates of [ $^3$ H]thymidine incorporation in H1299 cells at various times after treatment with two different doses of UVC light. As shown in Fig. 8*A*, the rates of DNA synthesis were reduced by 70% 2–4 h after irradiation with 2.5 J/m $^2$  UVC light, but recovered to control levels 8 h post-treatment. In contrast, after high dose UVC treatment (25 J/m $^2$ ), the rates of DNA synthesis were reduced to  $\sim$ 3% of control levels and did not recover. Therefore, the kinetics of inhibition and recovery of DNA synthesis in response to  $<$ 100 nM BPDE and 2.5 J/m $^2$  UVC light are very similar.

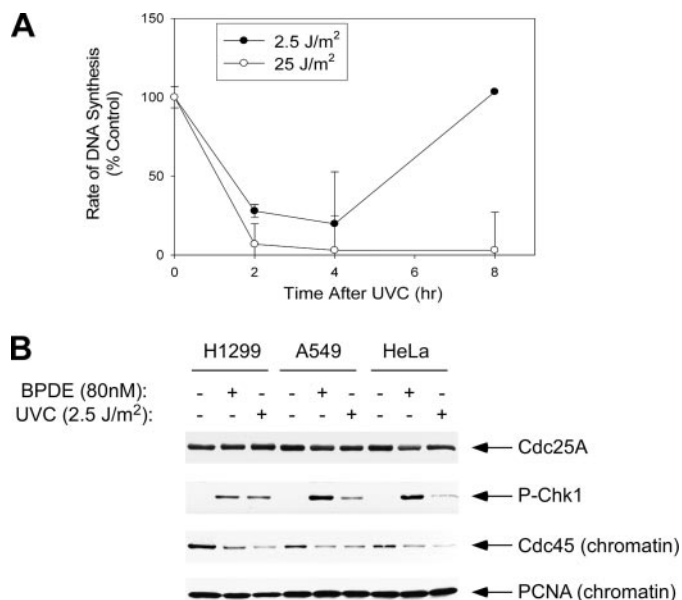
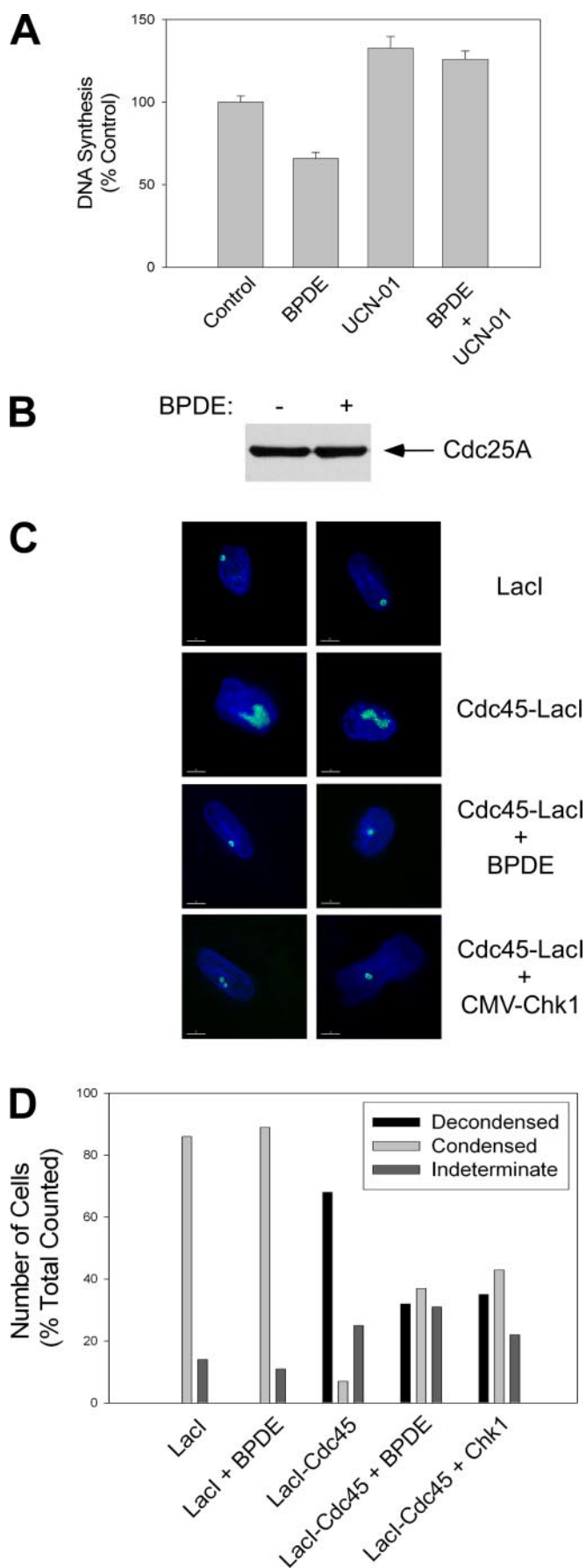


**FIGURE 8. Effect of UVC treatment on DNA synthesis, Cdc25A levels, and the chromatin association of Cdc45.** *A*, H1299 cells were irradiated with 2.5 or 25 J/m<sup>2</sup> UVC light or were left untreated as a control. At different time points after UVC treatment, the rates of DNA synthesis were determined by measurements of [<sup>3</sup>H]thymidine incorporation. *B*, H1299, A549, and HeLa cells were treated with 80 nM BPDE or 2.5 J/m<sup>2</sup> UVC light. 2 h later, the resulting cells were separated into soluble and chromatin fractions. After normalizing for protein content, the levels of Cdc25A, phospho (P)-Chk1 (Ser<sup>317</sup>), Cdc45, and PCNA were detected by immunoblotting.

We determined the effect of UVC light on Cdc25A levels and the chromatin association of Cdc45. As shown in Fig. 8*B*, treatments with 80 nM BPDE and 2.5 J/m<sup>2</sup> UVC light both caused decreases in the levels of chromatin-bound Cdc45, but did not affect Cdc25A expression. Therefore, BPDE and UVC light elicit similar checkpoint responses that target Cdc45 in a Cdc25A-independent manner.

We then investigated whether BPDE and UVC light elicit similar checkpoint responses in other cell lines. Therefore, H1299, A549, and HeLa cells were treated with 80 nM BPDE or 2.5 J/m<sup>2</sup> UVC light. As shown in Fig. 8*B*, these low doses of BPDE and UVC light decreased the chromatin association of Cdc45 (concomitantly with Chk1 phosphorylation) in a Cdc25A-independent manner in all three cell lines. Taken together, our data suggest that loss of chromatin-associated Cdc45 represents a general mechanism for the S-phase checkpoint induced by bulky lesions.

**FIGURE 7. Effect of BPDE and Chk1 on Cdc45-induced chromatin decondensation.** *A*, A03\_1 cells were treated with 60 nM BPDE and/or 150 nM UCN-01 as indicated. 2 h after treatments, the rates of DNA synthesis were determined by measurements of [<sup>3</sup>H]thymidine incorporation. *B*, in an experiment conducted in parallel with the DNA synthesis assays shown in *A*, control and BPDE-treated cells were lysed and analyzed for Cdc25A levels by immunoblotting. *C*, A03\_1 cells growing exponentially on glass slides were transiently transfected with an expression plasmid encoding LacI or LacI-Cdc45. In parallel cultures, cells were cotransfected with an expression vector for Chk1. 24 h post-transfection, some cultures were treated with 100 nM BPDE for 2 h prior to fixing with formaldehyde. The fixed cells were stained with anti-LacI antisera and visualized by immunofluorescence microscopy as described under "Materials and Methods." Representative cells exhibiting BPDE- and Chk1-induced changes in chromatin condensation are shown. *D*, cells containing condensed, decondensed, and indeterminate chromatin at the *lac* operator/dihydrofolate reductase locus were enumerated. 200 cells were examined for each experimental condition.

## S-phase Checkpoint Regulation of Cdc45

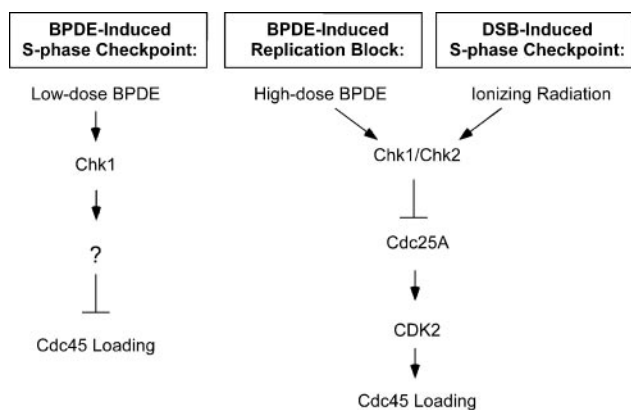


**FIGURE 9. Model of the distinct mechanisms of Cdc45 regulation in response to low and high levels of BPDE adducts and IR-induced DSBs.** Low levels of BPDE adducts inhibit Cdc45 loading in a Chk1-dependent manner that does not involve changes in Cdc25A and Cdk2. In contrast, high levels of DNA adducts that cause global replication blocks or IR-induced DSBs activate Chk1 and Chk2 and target Cdc25A for degradation. The resulting inhibition of Cdk2 activity prevents Cdc45 loading at unfired origins.

### DISCUSSION

Failure to properly integrate the biological responses after DNA damage and to accurately duplicate the human genome results in genetic instability, a hallmark of cancer (51, 52). The BPDE-induced S-phase checkpoint is likely to be important for maintaining genomic stability and preventing cancer after benzo[*a*]pyrene exposure. In this study, we have investigated the molecular basis of the intra-S-phase checkpoint elicited by BPDE-adducted DNA. Previous studies suggested that Cdc25A/Cdk2 and Cdc7/Dbf4 represent targets of checkpoint signaling cascades triggered by DNA damage in S-phase (13, 15, 25, 27, 42). Therefore, we tested the roles of Cdc25A, Cdk2, and Cdc7/Dbf4 in responses to BPDE-induced DNA damage. Similar to previous studies from other laboratories that used different genotoxins, we found that high doses of BPDE reduce Cdc25A levels, inhibit Cdk2 activity, and perturb association between Cdc7 and Dbf4. However, low concentrations of BPDE that inhibit initiation of DNA synthesis (*i.e.* activate the S-phase checkpoint) but do not affect global elongation fail to elicit detectable changes in Cdc25A, Cdk2, or Cdc7/Dbf4 association. Consistent with this finding, we have shown that the levels of Cdc25A, Cdk2, and Cdc7/Dbf4 are not rate-limiting for DNA synthesis when initiation is inhibited by low doses of BPDE. We suggest that Cdc25A, Cdk2, and Cdc7/Dbf4 are affected in response to global replication blocks (because of high levels of BPDE) or DNA DSBs (Fig. 9).

It is well established that the S-phase checkpoint response to bulky adducts (such as those induced by BPDE and UV light) is Chk1-mediated (4, 11). It is also accepted that Chk1 is a negative regulator of Cdc25A stability and thus of Cdk2 activity (13). Therefore, it is surprising that the BPDE-induced (Chk1-mediated) inhibition of DNA synthesis occurs without changes in Cdk2 activity. One possible explanation is that inhibition of Cdc25A by Chk1 requires a critical threshold level (or duration) of Chk1 signaling that exceeds the transient and modest Chk1 response induced by low doses of BPDE. We showed previously that 600 nM BPDE induces a higher level and more sustained phosphorylation of Chk1 than is evident in cells treated with

60–100 nM BPDE (4). It is also possible that additional signaling events induced by high doses of BPDE contribute to Cdc25A down-regulation. For example, we showed that Chk2 is phosphorylated in response to 600 nM BPDE, but not after treatment with 60 nM BPDE under conditions that activate the S-phase checkpoint. The DSB-induced intra-S-phase checkpoint involves Chk2-mediated amplification of Chk1-dependent systems (18). Therefore, efficient Cdc25A degradation might require threshold levels of adducts or different forms of DNA damage (*i.e.* DSBs) that elicit more extensive Chk1 and Chk2 signaling (Fig. 8).

In addition to Cdk2, Cdc7 kinase is crucial for initiation of DNA synthesis. Studies in model organisms have provided evidence that Cdc7 is a target of intra-S-phase checkpoint signaling (25). Using biochemical assays in *Xenopus* extracts, Gautier and co-workers (27) showed that the association between Dbf4 and Cdc7 is perturbed in an ATR-dependent manner after etoposide treatment. Moreover, the addition of recombinant Dbf4 enables DNA synthesis in etoposide-treated nuclei, demonstrating that Dbf4 is rate-limiting for DNA synthesis. It is unclear whether the concentrations of etoposide used in those experiments affected the initiation or initiation and elongation steps of DNA synthesis. We have shown here that inhibition of initiation or elongation has no effect on Cdc7 levels or its chromatin association. However, inhibition of elongation after treatment with high concentrations of BPDE inhibits the association between Cdc7 and ectopically expressed Dbf4. Unfortunately, because of the unavailability of antibodies, it has not been possible to perform similar experiments to determine the effect of S-phase checkpoint signaling on endogenous Dbf4 in human cells. However, antisera against murine Dbf4 are available, and we found that BPDE does not affect the levels of Dbf4 or its association with chromatin in mouse cell lines.<sup>3</sup> Moreover, we have shown that ectopic expression of Dbf4 (alone or in combination with Cdc7) does not prevent inhibition of DNA synthesis in response to BPDE. Therefore, in contrast with etoposide-treated *Xenopus* nuclei, Dbf4 levels are not rate-limiting for DNA synthesis in BPDE-treated cells. Recent studies suggest that immunodepletion of Dbf4 from *Xenopus* egg extracts fails to inhibit DNA synthesis (29, 53). Therefore, Dbf4 may not be the sole target of S-phase checkpoint signaling in etoposide-treated *Xenopus* extracts.

Using replication-competent *Xenopus* extracts, Dunphy and co-workers (28) have shown that Drf1, an alternative binding partner of Cdc7, associates with chromatin in response to agents that cause DNA damage and replication stress. These workers therefore suggested that Drf1 might be involved in S-phase checkpoint responses and that its association with chromatin could provide a mechanism for S-phase inhibition. ASKL1a and ASKL1c are splice variants of the mammalian Drf1 homolog (54). We tested the possible involvement of ASKL1a and ASKL1c in the S-phase checkpoint response to BPDE. We found that endogenous or overexpressed ASKL1a or ASKL1c did not associate with chromatin in response to DNA damage, in contrast with results from *Xenopus* extracts; moreover, high

<sup>3</sup> P. Liu, L. R. Barkley, and C. Vaziri, unpublished data.

level expression of ASKL1a or ASKL1c did not affect DNA synthesis in control or BPDE-treated cells.<sup>3</sup>

Therefore, we found no evidence that Dbf4 and ASKL1 have major roles in the BPDE-induced S-phase checkpoint in H1299 cells. However, it should be noted that we focused on responses to low doses of a specific lesion (BPDE adducts) under conditions in which replication initiation but not elongation is blocked. It is unclear if the concentrations of genotoxins used by Dunphy and co-workers (28) and Gautier and co-workers (27) affected elongation. Moreover, it is probable that different forms of DNA damage signal via different checkpoint mechanisms. Further experiments will be necessary to determine whether Dbf4 and ASKL1/Drf1 are involved in S-phase checkpoint responses to other forms of DNA damage in mammalian cells.

Because our analyses of Cdk2 and Cdc7 did not support roles for these kinases as targets of the BPDE-induced S-phase checkpoint, we investigated other potential mechanisms that might account for the effect of low doses of BPDE on DNA synthesis. The sequence of events involved in initiation of DNA replication is well understood. The assembly of pre-RCs (termed "licensing") begins in telophase and is completed after passage through G<sub>1</sub>. At the onset of S-phase, the actions of Cdk2 and Cdc7 result in recruitment of additional factors to the pre-RC. The first initiation factor recruited to the pre-RC is Mcm10. Mcm10 binding is necessary for recruitment of Cdc45 (45). Cdc45 is required in turn for origin unwinding and recruitment of replicative DNA polymerases (55). Cdc45 interacts with components of the pre-RC (including members of the Mcm2-7 complex, the putative replicative helicase) and DNA polymerases and might provide a physical bridge between initiation and elongation factors. We have shown here that BPDE inhibits the association of Cdc45 with chromatin concomitantly with activation of the S-phase checkpoint. Chromatin association with other replication factors (including Mcm10) is unaffected by BPDE, possibly indicating that checkpoint signaling inhibits initiation of replication at a step distal to Mcm10 recruitment but prior to Cdc45 loading.

In our experiments, BPDE-induced S-phase checkpoint signaling reduced the levels of chromatin-associated Cdc45 without affecting the large soluble pool (which comprises ~90% of total cellular Cdc45). Therefore, it is unlikely that the absolute levels of cellular Cdc45 are rate-limiting for DNA synthesis when the S-phase checkpoint is active. Indeed, Cdc45 overexpression did not abrogate the S-phase checkpoint.<sup>4</sup> Instead, BPDE-induced S-phase checkpoint signaling most likely inhibits the recruitment of Cdc45 to pre-RCs or stimulates the dissociation of Cdc45 from preinitiation complexes. The inhibition of chromatin decondensation induced by ectopically expressed LacI-Cdc45 in BPDE-treated A0\_31 cells also suggests a checkpoint mechanism mediated via decreased association of Cdc45 with chromatin.

Cdc45 has been proposed to tether polymerase  $\alpha$  to the RC during initiation via direct interactions with Mcm7 (47). The dissociation of Cdc45 from Mcm7 after BPDE treatment might

provide a mechanism for negative regulation of initiation of DNA synthesis by DNA damage signaling. Our finding that the interaction of Cdc45 with a defined origin of replication ( $\beta$ -globin) is perturbed in BPDE-treated cells is also consistent with a role for Cdc45 as a target of DNA damage signaling during the S-phase checkpoint.

Although it is well known that Cdc45 loading requires Cdk2 (56), we have shown that inhibition of DNA synthesis by low doses of BPDE occurs in the absence of any changes in Cdk2 activity. Moreover, our overexpression studies showed that Cdk2 activity is not rate-limiting for DNA synthesis in response to low doses of BPDE. Therefore, checkpoint signaling inhibits Cdc45 loading via a Cdk2-independent mechanism. Interestingly, there is a precedent for regulation of Cdc45 independent of changes in Cdk or Cdc7 activity. For example, in *Xenopus* extracts, Cdc45 is loaded onto chromatin in a *Xenopus* Mus101-dependent fashion that does not require pre-RC components or Mcm10 (57). The mammalian homolog of *Xenopus* Mus101 is the checkpoint protein TopBP1, which is already known to be required for Chk1-mediated checkpoint signaling (58–60). However, the role of TopBP1 in regulating initiation of DNA synthesis or Cdc45 loading in mammalian cells has not yet been studied. It is possible that changes in TopBP1-dependent Cdc45 loading could account for the effects of BPDE that we observed. It has been reported that protein phosphatase 2A is also necessary for Cdc45 loading (61). Using *Xenopus* extracts, Walter and co-workers (61) showed that ablation of protein phosphatase 2A inhibits chromatin loading of Cdc45 without affecting Cdk2 or Cdc7. Interestingly, protein phosphatase 2A is already known to be negatively regulated by the ATM pathway in response to IR (62). Potentially, a similar checkpoint-dependent inhibition of protein phosphatase 2A by the ATR/Chk1 pathway could provide a Cdk2/Cdc7-independent mechanism for inhibiting origin firing in response to low doses of BPDE.

In conclusion, we have demonstrated that Cdc45 is a likely target of the S-phase checkpoint induced by bulky lesions and that checkpoint-mediated inhibition of Cdc45/Mcm7 interactions occurs via a Cdk2-independent mechanism. Further studies are under way to determine the molecular basis for inhibition of Cdc45 by the S-phase checkpoint.

*Acknowledgments*—We thank Dr. Hisao Masai for providing expression vectors for Cdc7, Drf1, and Dbf4 and antisera against murine Dbf4 and Drs. Bill Kaufmann and Tim Heffernan for help and advice with the manuscript.

## REFERENCES

1. Zhou, B. B., and Elledge, S. J. (2000) *Nature* **408**, 433–439
2. Sancar, A., Lindsey-Boltz, L. A., Unsal-Kacmaz, K., and Linn, S. (2004) *Annu. Rev. Biochem.* **73**, 39–85
3. Larner, J. M., Lee, H., Little, R. D., Dijkwel, P. A., Schildkraut, C. L., and Hamlin, J. L. (1999) *Nucleic Acids Res.* **27**, 803–809
4. Guo, N., Faller, D. V., and Vaziri, C. (2002) *Cell Growth & Differ.* **13**, 77–86
5. Conney, A. H. (1982) *Cancer Res.* **42**, 4875–4917
6. Dipple, A. (1995) *Carcinogenesis* **16**, 437–441
7. Dipple, A., Khan, Q. A., Page, J. E., Ponten, I., and Szeliga, J. (1999) *Int. J. Oncol.* **14**, 103–111
8. Cordeiro-Stone, M., Boyer, J. C., Smith, B. A., and Kaufmann, W. K. (1986)

<sup>4</sup> P. Liu and C. Vaziri, unpublished data.

## S-phase Checkpoint Regulation of Cdc45

- Carcinogenesis* **7**, 1775–1781
- Weiss, R. S., Leder, P., and Vaziri, C. (2003) *Mol. Cell Biol.* **23**, 791–803
  - Painter, R. B. (1985) *Mutat. Res.* **145**, 63–69
  - Heffernan, T. P., Simpson, D. A., Frank, A. R., Heinloth, A. N., Paules, R. S., Cordeiro-Stone, M., and Kaufmann, W. K. (2002) *Mol. Cell Biol.* **22**, 8552–8561
  - Busino, L., Chiesa, M., Draetta, G. F., and Donzelli, M. (2004) *Oncogene* **23**, 2050–2056
  - Sorensen, C. S., Syljuasen, R. G., Falck, J., Schroeder, T., Ronnstrand, L., Khanna, K. K., Zhou, B. B., Bartek, J., and Lukas, J. (2003) *Cancer Cell* **3**, 247–258
  - Sorensen, C. S., Syljuasen, R. G., Lukas, J., and Bartek, J. (2004) *Cell Cycle* **3**, 941–945
  - Busino, L., Donzelli, M., Chiesa, M., Guardavaccaro, D., Ganoth, D., Dorrello, N. V., Hershko, A., Pagano, M., and Draetta, G. F. (2003) *Nature* **426**, 87–91
  - Jin, J., Shirogane, T., Xu, L., Nalepa, G., Qin, J., Elledge, S. J., and Harper, J. W. (2003) *Genes Dev.* **17**, 3062–3074
  - Kanemori, Y., Uto, K., and Sagata, N. (2005) *Proc. Natl. Acad. Sci. U. S. A.* **102**, 6279–6284
  - Bartek, J., Lukas, C., and Lukas, J. (2004) *Nat. Rev. Mol. Cell Biol.* **5**, 792–804
  - Zhao, H., Watkins, J. L., and Piwnica-Worms, H. (2002) *Proc. Natl. Acad. Sci. U. S. A.* **99**, 14795–14800
  - Falck, J., Petrini, J. H., Williams, B. R., Lukas, J., and Bartek, J. (2002) *Nat. Genet.* **30**, 290–294
  - Masai, H., and Arai, K. (2002) *J. Cell. Physiol.* **190**, 287–296
  - Bousset, K., and Diffley, J. F. (1998) *Genes Dev.* **12**, 480–490
  - Montagnoli, A., Valsasina, B., Brotherton, D., Troiani, S., Rainoldi, S., Tenca, P., Molinari, A., and Santocanale, C. (2006) *J. Biol. Chem.* **281**, 10281–10290
  - Masai, H., Matsui, E., You, Z., Ishimi, Y., Tamai, K., and Arai, K. (2000) *J. Biol. Chem.* **275**, 29042–29052
  - Jares, P., Donaldson, A., and Blow, J. J. (2000) *EMBO Rep.* **1**, 319–322
  - Duncker, B. P., and Brown, G. W. (2003) *Mutat. Res.* **532**, 21–27
  - Costanzo, V., Shechter, D., Lupardus, P. J., Cimprich, K. A., Gottesman, M., and Gautier, J. (2003) *Mol. Cell* **11**, 203–213
  - Yanow, S. K., Gold, D. A., Yoo, H. Y., and Dunphy, W. G. (2003) *J. Biol. Chem.* **278**, 41083–41092
  - Takahashi, T. S., and Walter, J. C. (2005) *Genes Dev.* **19**, 2295–2300
  - Vaziri, C., Saxena, S., Jeon, Y., Lee, C., Murata, K., Machida, Y., Wagle, N., Hwang, D. S., and Dutta, A. (2003) *Mol. Cell* **11**, 997–1008
  - Bi, X., Slater, D. M., Ohmori, H., and Vaziri, C. (2005) *J. Biol. Chem.* **280**, 22343–22355
  - Cordeiro-Stone, M., Frank, A., Bryant, M., Oguejiofor, I., Hatch, S. B., McDaniel, L. D., and Kaufmann, W. K. (2002) *Carcinogenesis* **23**, 959–965
  - Izumi, M., Yanagi, K., Mizuno, T., Yokoi, M., Kawasaki, Y., Moon, K. Y., Hurwitz, J., Yatagai, F., and Hanaoka, F. (2000) *Nucleic Acids Res.* **28**, 4769–4777
  - Pollok, S., Stoepel, J., Bauerschmidt, C., Kremmer, E., and Nasheuer, H.-P. (2003) *Biochem. Soc. Trans.* **31**, 266–269
  - Rosenblatt, J., Gu, Y., and Morgan, D. O. (1992) *Proc. Natl. Acad. Sci. U. S. A.* **89**, 2824–2828
  - Alexandrow, M. G., and Hamlin, J. L. (2005) *J. Cell Biol.* **168**, 875–886
  - Li, G., Sudlow, G., and Belmont, A. S. (1998) *J. Cell Biol.* **140**, 975–989
  - Pacek, M., and Walter, J. C. (2004) *EMBO J.* **23**, 3667–3676
  - Aladjem, M. I. (2004) *Front. Biosci.* **9**, 2540–2547
  - Todorovic, V., Falaschi, A., and Giacca, M. (1999) *Front. Biosci.* **4**, D859–D868
  - Avni, D., Yang, H., Martelli, F., Hofmann, F., ElShamy, W. M., Ganesan, S., Scully, R., and Livingston, D. M. (2003) *Mol. Cell* **12**, 735–746
  - Mailand, N., Falck, J., Lukas, C., Syljuasen, R. G., Welcker, M., Bartek, J., and Lukas, J. (2000) *Science* **288**, 1425–1429
  - Bi, X., Barkley, L. R., Slater, D. M., Tateishi, S., Yamaizumi, M., Ohmori, H., and Vaziri, C. (2006) *Mol. Cell Biol.* **26**, 3527–3540
  - Falck, J., Mailand, N., Syljuasen, R. G., Bartek, J., and Lukas, J. (2001) *Nature* **410**, 842–847
  - Takeda, D. Y., and Dutta, A. (2005) *Oncogene* **24**, 2827–2843
  - Wohlschlegel, J. A., Dhar, S. K., Prokhorova, T. A., Dutta, A., and Walter, J. C. (2002) *Mol. Cell* **9**, 233–240
  - Kukimoto, I., Igaki, H., and Kanda, T. (1999) *Eur. J. Biochem.* **265**, 936–943
  - Gladden, A. B., and Diehl, J. A. (2003) *J. Biol. Chem.* **278**, 9754–9760
  - Sterner, J. M., Dew-Knight, S., Musahl, C., Kornbluth, S., and Horowitz, J. M. (1998) *Mol. Cell Biol.* **18**, 2748–2757
  - Syljuasen, R. G., Sorensen, C. S., Hansen, L. T., Fugger, K., Lundin, C., Johansson, F., Helleday, T., Sehested, M., Lukas, J., and Bartek, J. (2005) *Mol. Cell Biol.* **25**, 3553–3562
  - Kastan, M. B., and Bartek, J. (2004) *Nature* **432**, 316–323
  - Nyberg, K. A., Michelson, R. J., Putnam, C. W., and Weinert, T. A. (2002) *Annu. Rev. Genet.* **36**, 617–656
  - Petersen, P., Chou, D. M., You, Z., Hunter, T., Walter, J. C., and Walter, G. (2006) *Mol. Cell Biol.* **26**, 1997–2011
  - Yoshizawa-Sugata, N., Ishii, A., Taniyama, C., Matsui, E., Arai, K., and Masai, H. (2005) *J. Biol. Chem.* **280**, 13062–13070
  - Walter, J., and Newport, J. (2000) *Mol. Cell* **5**, 617–627
  - Walter, J. C. (2000) *J. Biol. Chem.* **275**, 39773–39778
  - Van Hatten, R. A., Tutter, A. V., Holway, A. H., Khederian, A. M., Walter, J. C., and Michael, W. M. (2002) *J. Cell Biol.* **159**, 541–547
  - Parrilla-Castellar, E. R., and Karnitz, L. M. (2003) *J. Biol. Chem.* **278**, 45507–45511
  - Garcia, V., Furuya, K., and Carr, A. M. (2005) *DNA Repair* **4**, 1227–1239
  - Furuya, K., Poitelea, M., Guo, L., Caspari, T., and Carr, A. M. (2004) *Genes Dev.* **18**, 1154–1164
  - Chou, D. M., Petersen, P., Walter, J. C., and Walter, G. (2002) *J. Biol. Chem.* **277**, 40520–40527
  - Guo, C. Y., Brautigan, D. L., and Larner, J. M. (2002) *J. Biol. Chem.* **277**, 4839–4844